Proceedings of 10th IOE Graduate Conference
Peer Reviewed
ISSN: 2350-8914 (Online), 2350-8906 (Print)
Year: 2021 Month: October Volume: 10

Vulnerability Assessment of a Hybrid Masonry Building with Unreinforced Masonry Peripheral Walls and Central Reinforced Concrete Columns

Pranav Acharya[a], Gokarna B. Motra [b], Kshitij C. Shrestha [c] Arun Paudel[d]

[a, b, c, d] *Department of Civil Engineering, Pulchowk Campus, IOE, Tribhuvan University, Nepal*
Corresponding Email: [a] acharyapranav01@gmail.com, [b] gmotra@ioe.edu.np, [c] kshitij.shrestha@pcampus.edu.np, [d] arun.paudel@pcampus.edu.np,

Abstract
The practice of unreinforced masonry has been around since ages. In seismically active zones like Nepal, it is utmost for the structures to be designed by following proper seismic design criteria. But, most of the older unreinforced buildings in Nepal are non-engineered to semi engineered structures, which lack proper seismic detailing. A detailed visual assessment of the Panauti municipality area, led to the identification of a unique building typology. The typology has centrally located reinforced concrete columns supporting concrete slabs and beams spanning along the grid of columns which altogether rested over peripheral load bearing unreinforced brick masonry in cement mortar. The building was modelled in SAP2000 and pushover analysis was performed. This was followed by generation of fragility curves under different Peak Ground Accelerations(PGAs) of response spectra in IS 1893:2016 and NBC 105:2020.The fragility curves thus obtained were used to understand the vulnerability of the structure to considered earthquakes. This study can be further used for seismic assessment of similar typology buildings and for appropriate recommendation of strengthening measures.

Keywords
Unreinforced Masonry, NL Links, Link element, Capacity spectrum, Fragility generation

1. Introduction

Unreinforced masonry has been the face of an affordable and cost-effective housing construction technique in the context of Nepal. High vulnerability to earthquakes creeps in inevitably with this form of construction owing to the multitude of critical points within such structures and thus these structures are found to be more vulnerable to damage during earthquake shaking. Throughout its history, Nepal has experienced six great damaging earthquakes in the years 1255, 1408, 1505, 1833, 1934, and 2015 AD with magnitudes greater than or equal to 7.6 [1] . The 2015 Gorkha Earthquake of Magnitude 7.8 in Nepal damaged about 700,000 buildings. The distribution of building typologies in 31 districts, which were severely affected by the 2015 earthquake in Nepal shows that about 58% of the buildings are mud-based masonry(stone in mud, adobe or brick in mud), while 21% are cement based masonry(stone with cement-sand mortar or brick with cement-sand mortar) and about 15% are RC frame structures with masonry infill while the rest covering only 6% of the typologies [2]. According to the National Reconstruction Authority (NRA)[3], out of a total of 1,047,261 damaged houses surveyed, 78.4 percent belonged to low strength masonry, 7.87 percent were cement-mortared masonry and around 3.57 percent were reinforced concrete buildings. As Nepal lies in high risk of seismic activity, with frequent earthquakes, the buildings in Nepal need to be designed and constructed for proper earthquake resistance. However, older masonry structures of Nepal are mostly non-engineered and semi-engineered which basically lack seismic resistant detailing. Nepal has witnessed severe damage to buildings and significant loss of human lives in the past earthquakes. The damages caused by the earthquakes in the past demonstrate the vulnerability of buildings in Nepal [4]. It is thus important to take control on the factors that would tend to help minimize the earthquake damages in future. Paudel et. al.[5] presented a case study on strengthening of a masonry building inside Pulchowk Campus, which was severely damaged during 2015 Gorkha earthquake, in which RC jacketing was proposed as the most favorable option for strengthening the considered building. Maharjan et. al. [6] developed fragility curves to identify vulnerabilities to different time history records. Sah et. al. [5] used 3D FEM modeling and proposed retrofitting strategies for Shital Niwas building. Guragain et. al.[7] obtained fragility functions for non-engineered low earthquake resistant masonry buildings in Nepal.

The detailed visual assessment of the Panauti municipality area under the "Nepal Homes and Communities, Baliyo Ghar, Baliyo Sahar" project led to the identification of a unique building typology in the Panauti area. The identified typology has one or two centrally located RCC columns that support concrete slabs and beams spanning along the grid of columns which altogether rested over load bearing brick masonry in cement mortar over the periphery of building. This form of construction practice prevailing in this area helps to infer that people believe in taking some strengthening measures through the use of RCC columns without which it would simply be a load-bearing masonry wall system. However, this form of construction can be critical in the face of strong ground shaking. It is thus important to assess the seismic behavior of these structures and provide appropriate strengthening measures. In this paper, the analysis of one of the representative building models with the typology as explained earlier is done. Firstly, static analysis of the masonry building is done using 3D simplified macro modelling approach. Then, nonlinear links have been introduced according to the predefined conventional crack patterns in the walls and pushover analysis is performed to study its nonlinear behavior in in-plane direction. Further, fragility curves are generated to check seismic vulnerability levels of the prototype building.

2. Numerical simulation

2.1 Modelling techniques in Masonry

A detailed finite element approach, could be extremely time consuming during both the modelling and the result interpretation phases depending upon the complexity of the model[8]. The modeling strategies that are used for masonry[9, 10] are as shown in fig.1.

Detailed micro-modeling:
The interface between bricks and mortar is modeled by special elements that represent the discontinuities. The detailed micro-modeling approach is suited for smaller structural elements wherein the heterogeneity in the stress and strain is to be studied extensively.

Simplified micro-modeling:
The mortar joints and interface elements are re-defined as individual elements to represent a contact area. The masonry is treated as a set of continuum elements representing brick units bonded by potential fracture lines at the interface. The study of in-plane behavior of masonry walls has been done by a lot of researchers through this technique.

Macro-modeling:
The masonry panel is considered as a homogeneous element and this type of model reproduces the general structural behavior of a masonry panel. This approach is suitable when the structure being analysed is composed of solid walls with dimensions big enough that the stresses across the dimensions are more or less uniform.

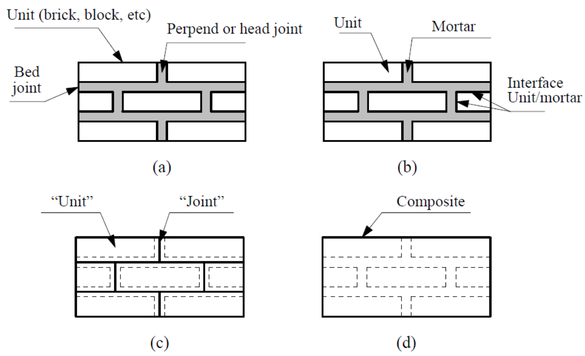

Figure 1: Modelling techniques in masonry (a) Masonry sample; (b) detailed micro-modeling; (c) simplified micro- modeling; (d) macro-modeling

2.2 NL Link elements

The Non-Linear (NL) link element allows the modelling of material nonlinearity by means of user defined force-deformation relationships. The area elements representing the interface of wall segments, where yielding is likely to occur, are replaced with nonlinear links. The area elements outside the assumed yielding regions are modeled with linear-elastic area elements using full gross-section properties[11]. The force-deformation relationships assigned to the nonlinear links, to represent both axial and shear behavior, are defined in terms of Multilinear

Plastic link elements. The force deformation relationship depends on the tributary area of wall elements represented by each of the nonlinear links. The axial deformation is defined by longitudinal direction of the link elements(fig.2) while the shear behavior is defined by the in-plane transverse direction(fig.3) [11].

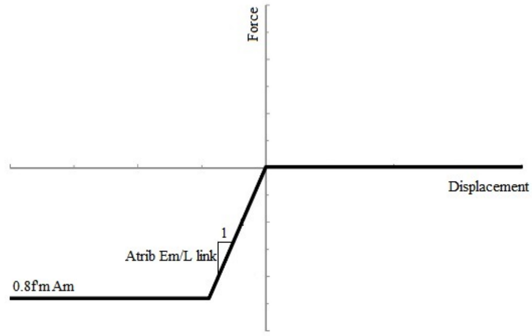

Figure 2: Non - Linear Link Definition for URM wall: Axial Direction

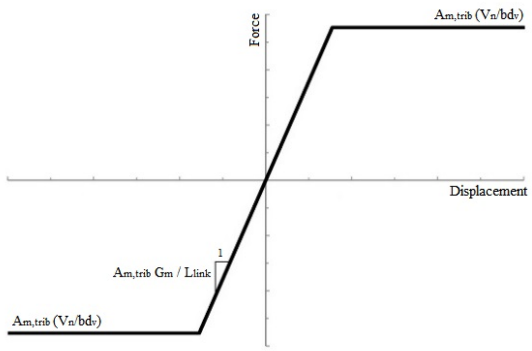

Figure 3: Non - Linear Link Definition for URM wall: Shear Direction

For representing the shear behavior, the force-deformation relationships are defined as bilinear and symmetrical (fig.3). The inclined line is defined by the stiffness of gross-section of the masonry and the horizontal portion represents the nominal shear strength. The effects of secondary moment are only assigned to one end of the link. To incorporate this in the model, a rigid line element is used at one end of the links throughout the considered wall section.

The following parameters have been used in the NL links in this paper. (fig.4,5, table.1, 2). Length and width of link = 0.25m, Cross sectional area of link = L x B [for vertical links, horizontally placed along length] and = B x H [for horizontal links, vertically placed along length]

Table 1: Axial Force-displacement plot: Bilinear

Displacement(m)	Force(kN)	Initial Stiffness
-0.00446	-235.75	
-0.00045	-235.75	529000 kN/m2
0	0	
0.00002	11.79	
0.00022	11.79	

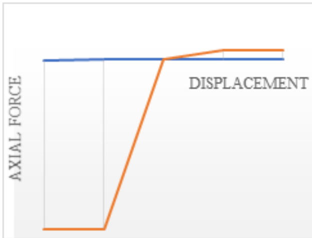

Figure 4: Bilinear force-displacement plot for Axial force

Table 2: Shear Force-displacement plot: Bilinear

Displacement(m)	Force(kN)	Initial Stiffness
-0.00068	-14.38	
-0.00007	-14.38	211600 kN/m2
0	0	
0.00007	14.38	
0.00068	14.38	

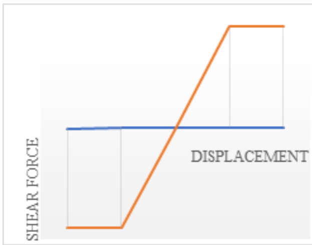

Figure 5: Bilinear force-displacement plot for Shear force

The links are placed at joints of meshed wall areas. The position of links have been chosen as seen in real buildings and by following the conventional crack patterns. The links are drawn as two joint links at corresponding joints. Depending on whether the joint lies at interior locations or at wall edges or edges of openings, the links that represented full tributary area and half the tributary area of a single brick unit are drawn respectively.

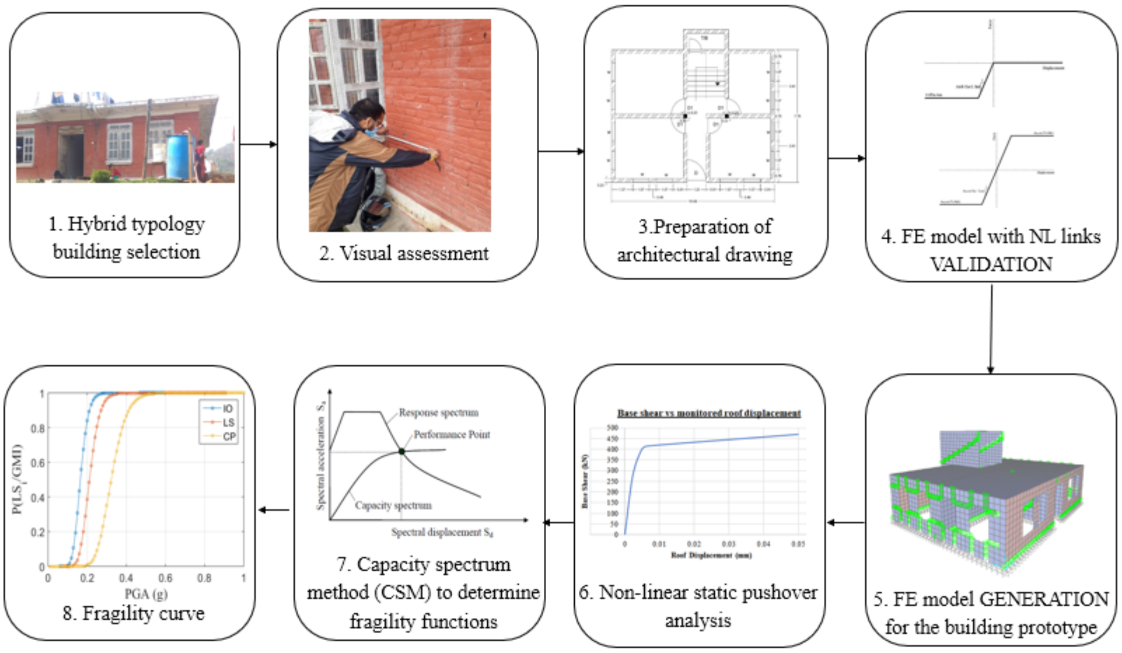

Figure 6: General methodology

3. Methodology

A building with centrally located RCC columns, beams and slabs with the beam and slab resting over peripheral load bearing brick masonry walls was selected and then different aspects of the building were visually examined. The important parameters of the building that are required for assessing its vulnerability are measured and recorded. Damages that have occurred in the building after the earthquake were also identified. The general methodology followed is shown in fig.6.

The collected data was then referred to prepare the building plans, elevations, sections; and a complete drawing was developed (fig.7) in Auto-CAD software which provided the basis for finite element modelling.

Table 3: General Building Description

Building Typology	Hybrid type with central RCC columns and peripheral load bearing masonry
No. of Stories	1.5
Storey height	2.75m
Building height	4.85
Plan dimensions	L = 10.52m, B = 8.76m
Floor	RCC Slab, M20
Walls	230mm thick brick walls (interior+ exterior)

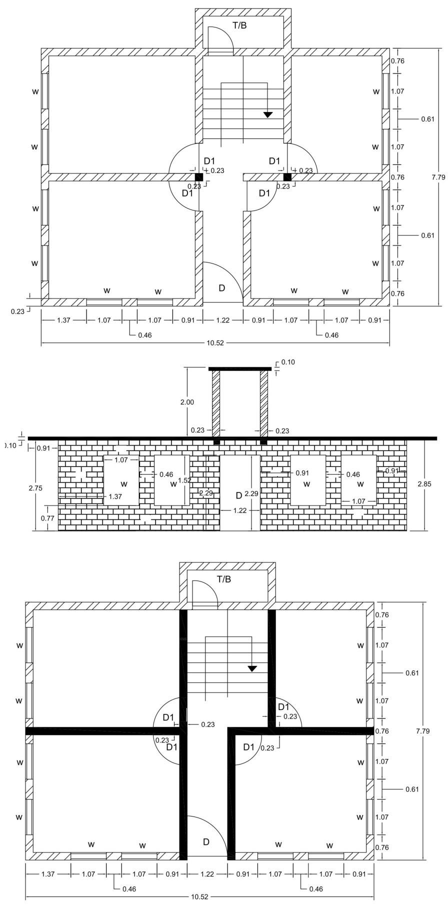

Figure 7: (a) Plan, (b) Elevation and (c) Beam Layout Plan

Figure 8: Pier cracks seen in selected building

Figure 9: Diagonal cracks seen in selected building

3.1 NL Links validation

Andres Lepage and Reynaldo E. Sanchez [11] proposed two modelling techniques: Nonlinear Layer Model and Nonlinear Link Model. In the Nonlinear Link model, the area elements at potential critical yielding sections are modified with nonlinear links. In their paper, the proposed simplified models are described through their application to a planar 2D one-story wall with two openings. In this paper, for accounting the non-linearity in the structure, the methodology proposed by Reynaldo and Sanchez, in the nonlinear link model has been followed. In the nonlinear link model proposed in the paper, the area elements representing the interface of wall segments, where yielding is likely to occur, are replaced with nonlinear links which are defined as Multilinear plastic. The user-defined force-deformation relationship is assigned to represent both axial and in-plane shear behavior of the yielding wall segments. The area elements outside the assumed yielding regions are modeled as linear-elastic area elements using full gross section properties.

For non-linear static analysis, a gravity load case is defined as a pre-load condition to determine the starting points on the force-deformation curves of each nonlinear link. The introduction of nonlinear links which would replace the area elements just like in the Reynaldo and Sanchez models were based on the visual assessment of the building under study. The links have been used in accordance with the observed crack patterns in the actual structure(fig.8,9). Also, frame auto hinges have been used at RCC column and beam junctions. The use of links in combination with frame hinges made it possible to account for the nonlinearity of the masonry structure under earthquake loadings.

3.2 Discontinuum Macromodeling in SAP2000

The modelling and analysis are conducted in the Finite Element Software, SAP 2000 v20.0.0. wherein 3D macro-modelling approach is adopted to model the current building under study. The masonry wall elements are modelled as thick shell and the roof slabs as thin shell area elements, meshed to 0.25x0.25m. The nonlinearities in the masonry wall system are represented by the use of non-linear link elements. The use of NL links was validated through previously published literature. Because of lack of actual field data and material testing, all mechanical properties of materials in the building are taken from relevant past literatures that account for the present study. The complete FE model has 2250 numbers of thick shell elements, 1203 numbers of thin shell elements, 9 numbers of frame element and 363 numbers of NL links. The materials properties of masonry and RCC are adopted from literature [12]. The concrete grade is used as M20, for beams, column and slabs and brick masonry in walls.

Table 4: Material Properties: Concrete

Concrete grade	M20
Young's Modulus (E)	22 GPa
Poisson's Ratio	0.2

Table 5: Material properties: Brick Masonry in Cement Mortar (BCM)

Compressive Strength of Masonry	4.1 MPa
Young's Modulus	2,300 MPa
Poisson's ratio	0.25
Modulus of Rigidity	920 MPa
Shear Strength	0.25 MPa

(Source: Kaushik et. al. [12])

Table 6: Frame sections

Name of frame section	Size
Beam	0.19m*0.23m
Column	0.23m*0.23m
Rigid line element	0.02m*0.02m

Table 7: Area sections

Name of area section	Thickness	Type
Slab	100mm	Thin shell
Wall	230mm	Thick shell

3.3 Position of links

Conventional crack patterns were considered and the observed crack locations(fig.8,9) were noted during visual assessment; on the basis of which links have been positioned ((fig.10,11,12)to account for the non-linearity.

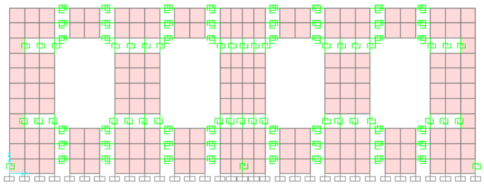

Figure 10: In-plane links in pier

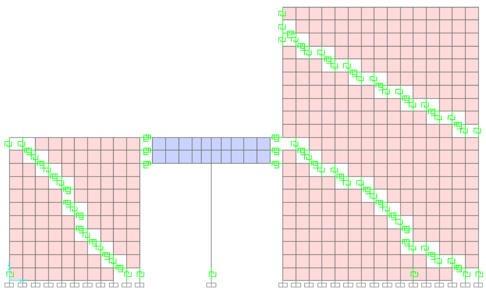

Figure 11: In-plane links along diagonal

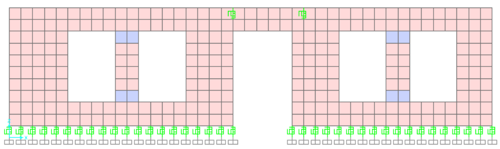

Figure 12: Out-of-plane links at toe

4. Results and Discussion

4.1 Linear Static Analysis

Results of static analysis gave the fundamental time period of building as 0.077seconds. The total mass participation in the first three modes was around 77% in Y direction.

4.2 Pushover Analysis

The building model is subjected to nonlinear static pushover analysis. For brevity and simplicity, pushover in Y direction is only performed. This direction represents the weaker side of the building with presence of majority of openings along the in-plane loaded walls. Pushover curve thus obtained is as shown in fig.13.

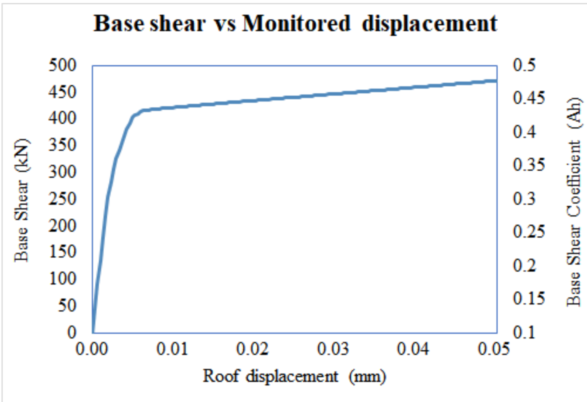

Figure 13: Base shear vs monitored displacement

4.3 Capacity Spectrum Method (CSM)

The Capacity Spectrum Method(CSM) compares the two major elements of performance based design viz., Capacity and Demand. Capacity is the ability of the structure to resist the earthquake demand.

Conversion of Capacity curve to Capacity Spectrum (in ADRS):

The pushover (capacity) curve expressed in terms of base shear vs roof displacement is converted into capacity spectrum. The capacity spectrum is simply the capacity curve in the Acceleration-Displacement Response Spectra format (ADRS).

$$S_A(T) = \frac{V_B}{M} \tag{1}$$

Where, V_B represents the seismic Base Shear, and M

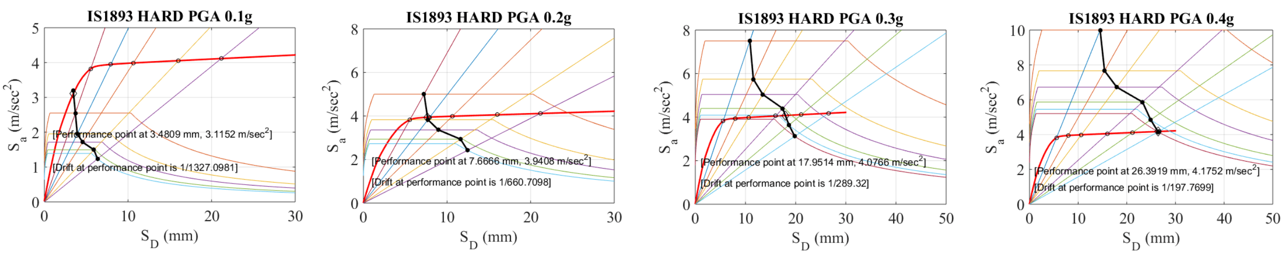

Figure 14: Comparison of performance points at different PGA values as per IS1893:2002 for hard soil)

is the Effective Modal Mass given as:

$$M = \frac{L_n^2}{M_n} = \frac{(\sum m_i(\delta_{i1}))^2}{\sum m_i(\delta_{i1})^2} \tag{2}$$

$$S_D(T) = \frac{(\delta_{i1})^T[m](\delta_{i1})}{((\delta_{i1})^T[m](1)} \tag{3}$$

Where, $(\delta)_1 = (\phi)_1 \beta_1 S_D(T)$ is the displacement vector of first mode and [m] is the lumped floor mass matrix.

Conversion of response spectrum to Demand Spectrum (in ADRS):
Two response spectra from IS 1893:2016 [13] and NBC 105:2020 [14] were chosen for this study. The input response spectrum (SA - T format) is then converted into ADRS format (SA - SD) by using the relation:

$$S_D(T) = (\frac{T}{2\pi})^2 S_D(T) \tag{4}$$

The performance points were then calculated according to the procedure as proposed by Otani et. al.(2000) [15] through programming in MATLAB.

The performance points for different PGA levels of different sources of earthquake response spectra were then obtained.

The determination of performance point with different PGAs varying from 0.1g to 0.4g of IS 1893:2016 for hard soil response spectrums is shown in fig.14. The storey drift at corresponding performance points is higher for increasing values of PGA from left to right.

4.4 Generation of Fragility Curves

The fragility curve generation is one of the statistical tools that utilizes the results obtained from appropriate structural response assessment and helps analyse the vulnerability of the structure to different damage levels. Different values of performance points are obtained after the CSM analysis for various ground motion parameters. The fragility curve gives the probability of exceeding a specific damage level under earthquake intensity parameter, which in this case is Peak Ground Acceleration(PGA). Wen et al. (2004) [16] proposed a method of generation of fragility curves, which has been used in this paper. The probability of exceeding a limit-damage state for the given Ground Motion Intensity (GMI) is given as:

$$P(LS_i/GMI) = 1 - \phi(\frac{\lambda_{cl}^i - \lambda_{D/GMI}}{\beta_{D/GMI}}) \tag{5}$$

where, $\lambda_{D/GMI}$ is ln(calculated median demand storey drift from the best fit power law line) and $\beta_{D/GMI}$ is the demand uncertainty, which are given as:

$$\lambda_{D/GMI} = \ln(a_1) + a_2 \ln(GMI) \tag{6}$$

$$\beta_{D/GMI} = \sqrt{\frac{\sum_{K=1}^{n}[\ln(GMI_k) - \lambda_{GMI}(GMI_k)]^2}{n-2}} \tag{7}$$

Plotting of the natural log values corresponding to storey drift and PGA (fig.15)gives the values of the constants a1 and a2.

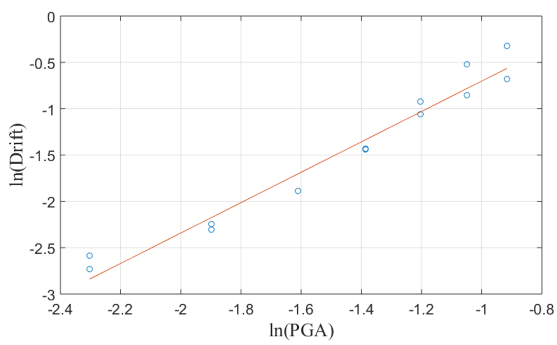

Figure 15: Regression plot

The limit states of: Immediate Occupancy (IO), Life safety (LS) and collapse prevention (CP) have been defined at 1⁄750 (i.e. 0.13% drift), 1⁄500 (i.e. 0.2% drift), and 1⁄250 (i.e.0.4% drift) for the generation of fragility curves. These defined limit states are comparable with the threshold values defined in FEMA 273 [17]. The fragility curve is thus obtained for different limit states as shown in fig. 16.

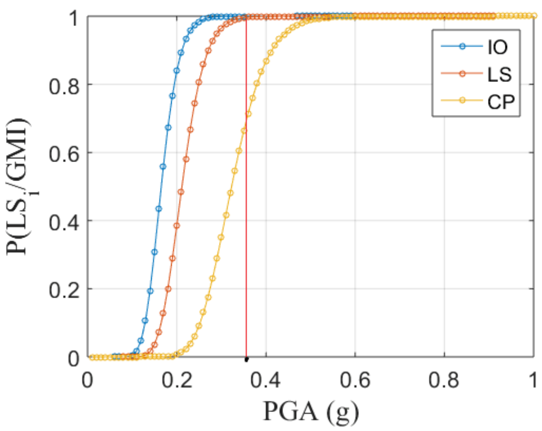

Figure 16: Fragility Curve

5. Conclusion and Recommendations

The fragility curves generated depict the vulnerability of the considered structure to earthquake shakings. For a PGA of 0.36g (the Maximum Considered Earthquake(MCE) in IS 1893:2016), the probability of exceeding the CP level is 70% while exceeding the IO and LS level is 100%. High vulnerability of the considered structure is thus evident. Further, more number of buildings with similar typology can be analysed for getting a clearer picture of the state of vulnerability of these typology buildings. Accordingly, the future works will focus on extending the current model to propose seismic retrofitting measures for the selected prototype URM building.

References

[1] Thapa D.R., Tao X., Wang G, and Fan F. Deterministic seismic hazard assessment for Nepal. In *Sixteenth World Conference on Earthquake Engineering Santiiago Chile*, 2017.

[2] Tiwari K., Pradhan S., Guragain R., and Shrestha H. Multiple analytical approaches on seismic retrofit design of unreinforced masonry buildings in Nepal. In *17th World Conference on Earthquake Engineering*, 2020.

[3] National Reconstruction Authority (NRA). *A Journal of Development. Vol-I. May*.

[4] Shrestha H.D., Subedi J., and Rajbhandari M. Seismic retrofitting guidelines of buildings in Nepal, 2016.

[5] Motra G.B. and Paudel S. Performance evaluation of strengthening options for institutional brick masonry buildings: A case study of Pulchowk Campus. *Progress in Disaster Science*, 2021.

[6] Maharjan A. and Parajuli H.R. Seismic performance evaluation of stone masonry houses constructed with reinforced concrete bands. *Nepal Journal of Science and Technology (NJST*, 2020.

[7] Guragain R., Dixit A.M., and Meguro K. Development of fragility functions for low strength masonry buildings in nepal using Applied Element Method. In *15th WCEE Conference*, Lisboa, 2012.

[8] Andreini M., Caliò I., Cannizzaro F., De Falco A., Pantò B., Sassu M, and Giresini L. In *Seismic Assessment of The Historical Mixed Masonry-Reinforced Concrete Government Palace In La Spezia*. 2014.

[9] Lourenço P.B. Computational strategies for masonry structures, 1996.

[10] Campbell J. and Durán M. Numerical model for nonlinear analysis of masonry walls. *Revista de la construcción*, 2017.

[11] Sánchez Bravo R. *Limit Design of Reinforced Masonry Walls For Earthquake-Resistant Construction*. Phd thesis,, Pennsylvania State University, 2012.

[12] Kaushik H.B., Rai D.C., and Jain S.K. Stress-strain characteristics of clay brick masonry under uniaxial compression. *J. Mater. Civ. Eng*, 19(9):728–739,, 2007.

[13] IS1893. *Indian Standard Criteria for Earthquake Resistant Design of Structures-Part I: General Provisions and Buildings(Sixth Revision*. Bureau of Indian Standards, New Delhi, 2016.

[14] NBC105:2020. Nepal National Building Code: Seismic Design of Buildings in Nepal. *Department of Urban Development and Building Construction*, 2020.

[15] S. Otani, H. Hiraishi, M. Midorikawa, and M. Tashigawara. *New Seismic Design Provisions in Japan*. ACI Special Publication.

[16] Wen Y., Ellingwood B., and Bracci J. Vulnerability function framework for consequence-based engineering, 2004.

[17] FEMA - 273. *NEHRP Guidelines for the Seismic Rehabilitation of Buildings*.